Title:
Stochastic binding of Staphylococcus aureus to hydrophobic surfaces

Authors:
Nicolas Thewes, Alexander Thewes, Peter Loskill, Henrik Peisker, Markus Bischoff, Mathias Herrmann, Ludger Santen and Karin Jacobs

This is the accepted manuscript of an article published in *Soft Matter* (Volume 11(46), 2015, Pages 8913-8919, DOI: 10.1039/C5SM00963D).
The version of record is available online at: https://doi.org/10.1039/C5SM00963D

Journal Name

ARTICLE TYPE

Cite this: DOI: 10.1039/xxxxxxxxxx

Stochastic binding of *Staphylococcus aureus* to hydrophobic surfaces

Nicolas Thewes,[a] Alexander Thewes,[b] Peter Loskill,[a†] Henrik Peisker,[c] Markus Bischoff,[c] Mathias Herrmann,[c] Ludger Santen[b] and Karin Jacobs*[a]

Received Date
Accepted Date

DOI: 10.1039/xxxxxxxxxx

www.rsc.org/journalname

The adhesion of pathogenic bacteria to surfaces is of immense importance for health care applications. Via a combined experimental and computational approach, we studied the initiation of contact in the adhesion process of the pathogenic bacterium *Staphylococcus aureus*. AFM force spectroscopy with single cell bacterial probes paired with Monte Carlo simulations enabled an unprecedented molecular investigation of the contact formation. Our results reveal that bacteria attach to a surface over distances far beyond the range of classical surface forces via stochastic binding of thermally fluctuating cell wall proteins. Thereby, the bacteria are pulled into close contact with the surface as consecutive proteins of different stiffness attach. This mechanism greatly enhances the attachment capability of *S. aureus*. It, however, can be manipulated by enzymatically/chemically modifying the cell wall proteins to block their consecutive binding. Our study furthermore reveals that fluctuations in protein density and structure are much more relevant than the exact form of the binding potential.

The adhesion of bacteria to surfaces plays an important role for many processes in our everyday life: In the clinical setting, it can be the major factor for the transmission of diseases or the starting point of infectious biofilms on implants or catheters.[1,2] The fundamental reason for studying bacterial adhesion is mostly its prevention.[3,4] Yet, the majority of studies concentrate on the detachment process, mainly the adhesion force, which represents the maximum force acting between bacterium and colonized surface, in other words, it is studied how to get rid of already attached bacteria.[5–7] In our opinion, the first logical step to prevent bacterial adhesion, is to detain a bacterium from attaching and therefore, a fundamental understanding of the contact initiation process of a bacterium to a surface is crucial. In recent years, atomic force microscopy (AFM) was refined to perform force spectroscopy and is now established as a powerful and versatile method to characterise bacterial adhesion; especially the use of 'bacterial probes' allows for a precise and quantitative insight into the involved forces.[6,8–11] 'Bacterial probes' are AFM cantilevers, for which the tip is replaced by a single bacterium or a consortium of bacteria.

Interaction forces that arise in AFM force spectroscopy while the probe is continuously approached to the surface lead to a deflection of the cantilever. The deflection is monitored by a laser beam reflected from the back of the cantilever to a position-sensitive photodiode. Under quasistatic conditions, cantilever deflection is a measure of the force between tip and surface. However, a classic force curve features unstable points if, in a certain range, the gradient of the interaction force between tip and surface exceeds the cantilever spring constant. This leads to an abrupt change of the cantilever deflection, and the tip/surface separation.[12] Assuming a Lennard-Jones-like interaction potential, one instability occurs during the approach part of the force/distance curve and is called 'jump-to-contact' or 'snap-in'. A detailed analysis is given by Y. Seo and W. Jhe.[8] However, recent findings indicate that with a viable bacterial probe, the snap-in can also be a rather extended event (in range and time) than a sudden jump into contact.[13] The phenomenon can be described by a model for bacterial adhesion that involves the consecutive attachment of bacterial cell wall macromolecules to the substratum (for example, due to hydrophobic interactions). It was hypothesised that the form (depth and width) of the snap-in event is characteristic of the adhesive molecules of a bacterium.[13] In this study, we provide experimental evidence for this model, by demonstrating that the form of the snap-in event is defined by properties of the cell wall proteins. The snap-in process becomes more pronounced as the surface energy of the substratum becomes smaller, therefore we concentrate in this study on low-

[a] *Experimental Physics, Campus E2 9, Saarland University, D-66123 Saarbrücken, Germany. E-mail: k.jacobs@physik.uni-saarland.de*
[b] *Theoretical Physics, Campus E2 6, Saarland University, D-66123 Saarbrücken, Germany*
[c] *Institute of Medical Microbiology and Hygiene, Saarland University, D-66421 Homburg/Saar, Germany*
† Present address: Dept. of Bioengineering and California Institute for Quantitative Biosciences (QB3), University of California at Berkeley, Berkeley, California 94720, USA

energy surfaces such as hydrophobised silicon (Si) wafers.

We investigated the initiation of contact between exponential phase cells of *S. aureus* strain SA113 [14] and the hydrophobic surface of a silanised Si wafer. We additionally performed Monte Carlo (MC) simulations using a simple model for the adhesion of a bacterium to a surface. [13] By comparing experimental and simulated force/distance curves, we gained insight into the molecular mechanisms governing the initial attachment of *S. aureus*. Furthermore, by using bioactive agents that either crosslink or degrade proteins, properties of the cell wall can be altered in a controlled manner.

1 Material and Methods

Preparation of substratum

As substrates, we used Si wafers since they feature a very low roughness (0.09(2) nm) and are easily available in consistently good quality with a known surface chemistry. Si wafers (Siltronic AG, Burghausen, Germany) have a native silicon oxide layer (d=1.7(2)‡ nm). The wafers were rendered hydrophobic by self-assembly of a CH_3 terminated monolayer of OTS molecules following a standard protocol. [15] The hydrophobised Si wafers have a surface roughness of 0.12(2) nm and an advancing (receding) water contact angle of 111(1)° (107(2)°). Using polar/apolar liquids, the surface energy can be determined to be 24(1) mJ/m^2, [15] the streaming potential is -80.0(1) mV at pH 7.3. [10] For the force measurements, hydrophobised silicon wafers are immersed into 6 ml phosphate-buffered saline (PBS, pH 7.3, ionic strength 0.1728 mol/L at 20 °C).

Bacterial strain and growth conditions

S. aureus strain SA113 is a cell-invasive and biofilm-positive laboratory strain frequently used to study the functions of cell wall-anchored or -attached molecules of this pathogenic species. [16–19] Exponential growth phase *S. aureus* cells were freshly prepared for each experiment. 40 μl of an overnight culture were transferred into 4 ml Tryptic Soy Broth (TSB) medium and cultured at 37 °C and 150 rpm for 2.5 hours. To dilute the bacterial solution, 0.5 ml of the culture and additional 0.5 ml of PBS were inserted into a 1.5 ml microtube. To remove extracellular material, these bacteria were washed four times using 1 ml PBS each.

Preparation of bacterial probes

Single cell bacterial probes base on tipless cantilevers (MLCT-O, Bruker Nano, Santa Barbara, CA): Cantilevers were cleaned in an air plasma and vertically immersed for about 50 min into a solution allowing the polymerisation of dopamine, that is 4 mg/ml dopamine hydrochloride (99%) in 10 mM TRIS-buffer (pH 7.9 at 22 °C), both by Sigma Aldrich, Germany. During polymerisation, the cantilevers are stored in a fridge. Then, cantilevers were carefully rinsed with ultrapure water to remove unbound (poly)dopamine and dried under a laminar flow bench. Cantilever spring constants were determined before attaching a single bacterium using the thermal tune technique. [20] A single bacterium was attached using a micromanipulation system (Narishige Group, Japan) linked to an optical microscope: A droplet (approx. 30 μl) of diluted bacterial solution (see above) was placed on a polystyrene petri dish, were the bacteria are allowed to sediment. Then, the functionalised cantilever, mounted on the micromanipulator, is dipped into the droplet. By carefully tapping onto a single *S. aureus* cell with the upper end of the polydopamine-coated cantilever, the cell attaches to the cantilever. To safely exclude interactions between cantilever and substratum during the force measurements, the single bacterium should get attached as close as possible to the very end of the cantilever (not exceeding a distance of roughly two bacterial diameters). Subsequently, the cantilever is retracted from the droplet of bacterial solution and reintegrated into the AFM to perform force spectroscopy measurements. The inset to Fig. 2b depicts a single bacterial probe. To ensure that our method does not harm the cell, its viability can be checked after completing the measurements, using live/death staining (Life Technologies GmbH, Germany). Thereby, a small amount of live/death stain (20 μl) is added directly onto the bacterial probe and the viability of the bacterium is determined under a fluorescent light microscope (cf. supplementary material).

Force spectroscopy

All force/distance curves in this study were performed in PBS under room temperature on a Bioscope Catalyst AFM (Bruker Nano, Santa Barbara, CA). The cantilever was approached (and retracted) over a distance of 800 nm while 1024 data points were recorded for each part. The drive velocity was 400 nm/s and retraction started immediately after the chosen force trigger was reached on approach. Positive force triggers hereby reflect a net repulsive force, resulting in a 'standard' force distance/curve. Setting a negative force trigger allows to record 'partitioned' force/distance curves by switching from approach to retraction at the attractive part of the approach curve, as shown below.

2 Results and Discussion

Standard force/distance curves

A standard force/distance curve between a single *S. aureus* AFM probe and a hydrophobised Si wafer can be comprehended in terms of the properties of the bacterial cell wall (cf. schematic diagram in Fig. 1 and experimental curve in Fig. 2): In the case of *S. aureus*, the cell wall consists of numerous proteinaceous and non-proteinaceous macromolecules. [21,22] According to our model (as recently described for the apathogenic staphylococcal species *S. carnosus*, [13]) at a certain distance (called **'snap-in separation'**) above the wafer surface, the longest and/or most extended macromolecules start to interact with the wafer via short-range attractive forces§. Once tethered, the extended macromolecules tear the bacterium to the surface at point (1) in Fig. 2a or b. Along with that, more and more macromolecules can

‡ The number in the bracket denotes the standard deviation of the last digit.

§ In electrolyte solution (buffer), screening effects virtually lead to the absence of long-range forces. [23]

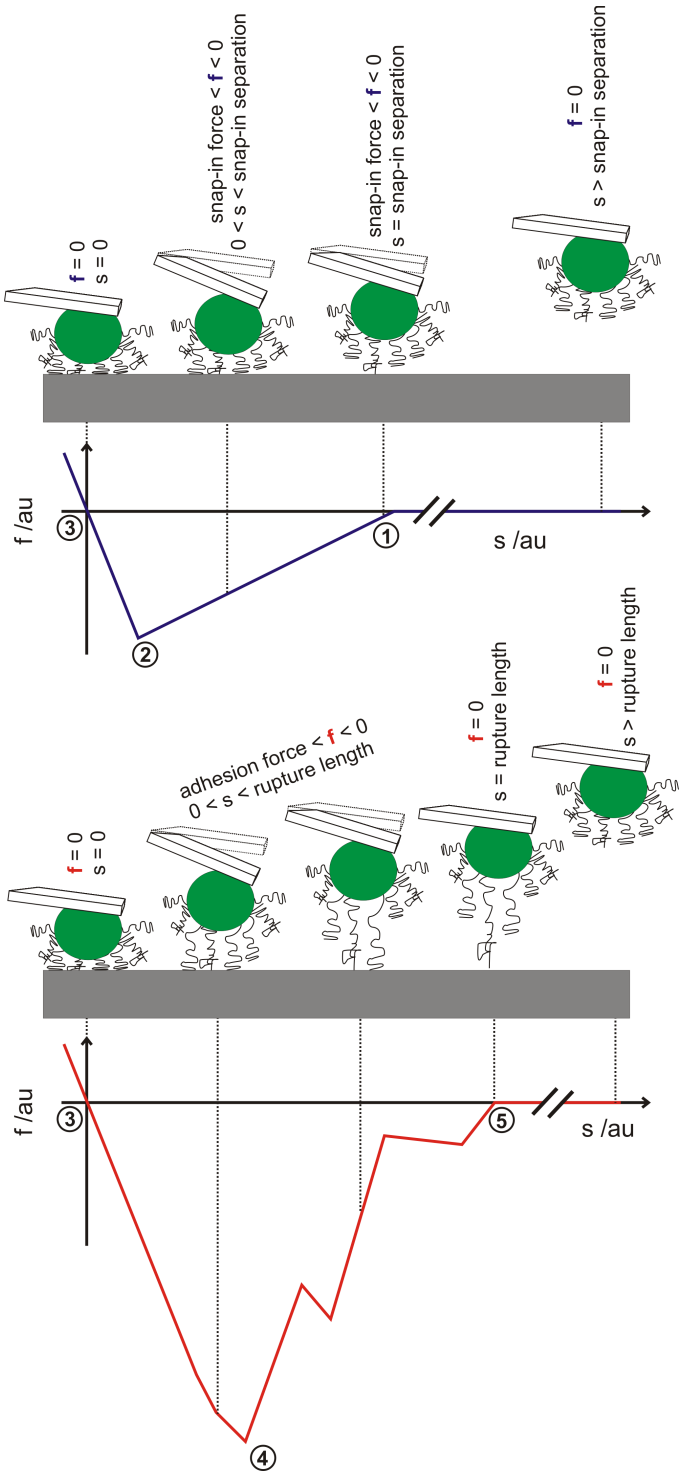

Fig. 1 Schematic diagram showing the bacterial adhesion process according to our model (approach in the upper sketch and retraction in the lower one). An additional sketch of a force/distance curve (with force f and separation s in arbitrary units au) indicates the link between the model-situation and the respective experimental force/distance signal, approach (retraction) in blue (red). Magnitudes do not reflect real situations.

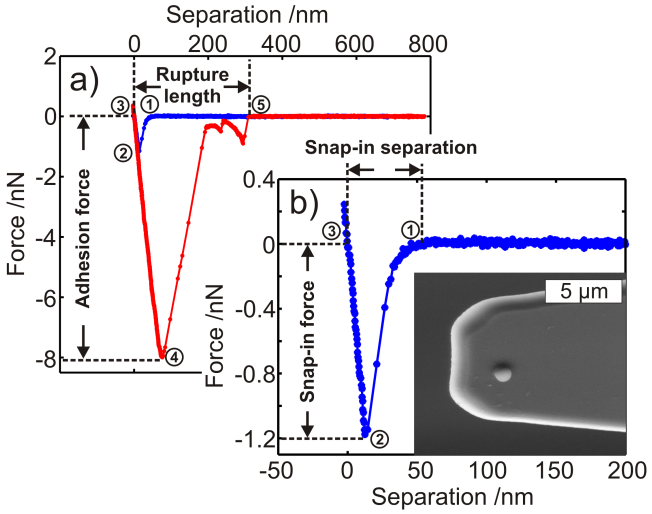

Fig. 2 Exemplary 'standard' force/distance curve recorded with a single *S. aureus* cell on a hydrophobised Si wafer and a positive force trigger of 300 pN (approach is displayed in blue and retraction in red). a) Entire curve, b) approach part of a) in more detail. The inset in b) shows an electron micrograph of the bacterial probe (radius of bacterium around 500 nm).

tether, yet some of the longest may therefore already be compressed. Fig. 2b demonstrates that the snap-in event is indeed an extended process, since dozens of data points can be recorded. The time between two data points is in the order of 10^{-3} s (defined by the force/distance curve parameters, see above). Soon, a point is reached where, with a further approach of the cantilever, more molecules are compressed than new macromolecules tether. Then, the minimum force of the snap-in process (the **'snap-in force'**) is reached (2) and a further approach mainly compresses the macromolecules. In a standard force/distance curve after crossing zero force (3), approach is stopped once the preset positive force trigger has been reached. Upon retraction, the compressed macromolecules are released, unfolded and/or stretched. Close to the force minimum (reflecting the **'adhesion force'**), the slope decreases, since more and more macromolecules start to detach (4). From now on, the number of attached molecules decreases that much that the measured force is more and more reduced. At a certain distance (called **'rupture length'**) the bacterium, viz. its cell wall macromolecules, detach completely (5). Depending on the type and number of the involved macromolecules, the retraction curve looks different for every individual single cell bacterial probe, a fact that has been found earlier in non-bacterial systems involving macromolecules.[24–27] The four measures of the force/distance curve (snap-in separation, snap-in force, adhesion force and rupture length) are usually very robust for one bacterial cell, as can be seen in an overlay of 20 force/distance curves with the same bacterial probe (cf. Fig. 3). For different cells, even of the identical bacterial culture, the four measures can vary markedly. However, by comparing a large number of cells, differences between bacterial species show up. For instance, the adhesion of the facultative pathogenic species *S. aureus* outperforms that of apathogenic *S. carnosus*.[13] In the

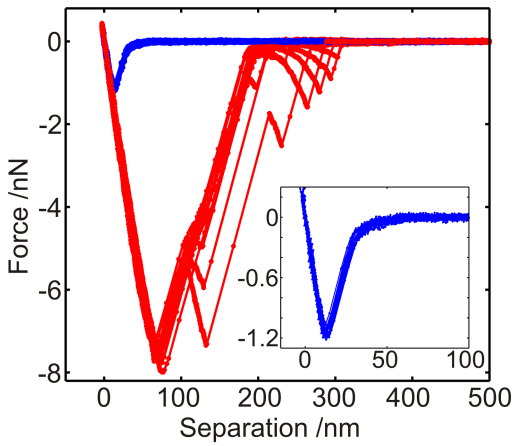

Fig. 3 Overlay of 20 standard force/distance curves showing the adhesion of a single *S. aureus* cell to a hydrophobised Si wafer. One of the curves was shown in detail in Fig. 2, approach (retraction) is market in blue (red), force trigger 300 pN. The snap-in process is shown in more detail in the inset.

exemplary curve, the snap-in separation is around 50 nm and the snap-in force is almost 1.2 nN. In the retraction part, discrete steps can frequently be observed which are similar to single molecule spectroscopy.[28]

Partitioned force/distance curves

In order to further explore the initial attachment of a bacterial cell, we focus on the nature of the snap-in event and the above mentioned partitioned force/distance curves. For this purpose, the force trigger is set to a negative value between the snap-in separation (1) and the snap-in force (2) displayed in Fig. 2, using the identical bacterial probe.

Fig. 4a shows an overlay of 20 partitioned force/distance curves with a force trigger of -100 pN. After stopping the approach, the piezo movement is immediately reversed and the bacterial probe is retracted. For -100 pN, the retraction curves did not resemble the ones of the standard force/distance curves shown in Fig. 3, as the adhesion force is greatly reduced. Nevertheless, these retraction curves feature the rupture length of the standard force/distance curve and a gradually reduced force. With decreasing force trigger (negative sign!) and, hence, a reduced distance of the bacterial probe to the surface (cf. Figs. 4b-d), the form and the adhesion force of the standard *S. aureus* force/distance curve is recovered. A closer look reveals that at a force trigger of -150 pN two out of the 20 force/distance curves resembled in their retraction part those of the standard force/distance curve and this ratio increased along with decreasing force trigger (Figs. 4b-d). Three characteristic features are noteworthy:

i) The retraction curves of the partitioned force/distance curves resemble the 'parallel and simultaneous stretching' of macromolecules independent of the applied negative force trigger.[25]

ii) With decreasing force trigger (negative sign; getting bacterium closer to the surface), the adhesion force does not increase gradually: Rather, either a low (less than one nN) or the 'standard' adhesion force is obtained. No intermediate force values are observed.

iii) Even if the piezo already moves the cantilever away from the surface, an increasing adhesive force is recorded, going along with a decreased separation between probe and surface (see Figs. 4b, c, d, red curve within in the dashed green circle), which we term 'pulling regime' in the following. It ends as soon as a minimum separation is reached. Upon further piezo retraction, the standard force/distance curve is recovered. For the low adhesion force, the pulling regime is absent.

These characteristics call for an interpretation in a molecular model: In this model, cell wall macromolecules are responsible for the initial attachment of the bacterium to the hydrophobic surface. A force trigger of only -100 pN (cf. Fig. 4a) is apparently insufficient to enable the attachment of a sufficient number and/or the right types of molecules to withstand the restoring force of the cantilever after piezo reversal. Thus, the separation between surface and bacterium increases immediately with cantilever retraction and neither a pulling regime nor a standard adhesion force are observed. Rather, this case is accompanied with a low adhesion force. In contrast, at force triggers of -150 pN and less, a pulling regime is observed, so the already attached macromolecules are strong enough to withstand the restoring force of the cantilever after piezo reversal, thereby facilitating the binding of additional macromolecules. Subsequently, the bacterium is pulled closer to the surface against cantilever retraction. The pulling regime ends at the point where the net attractive force of the cell wall macromolecules is outmatched by the restoring force of the cantilever and, thereby, further approach is prevented. Then, the standard retraction curve and adhesion force is recovered.

In Figs. 4b and c, both types of adhesion forces are recorded, which is due to the stochastic nature of the molecular processes involved during contact initiation.[13] In Fig. 4d, no low adhesion force curves were measured, which corroborates the above argument that at larger negative force triggers, more and more molecules are able to tether, giving rise to maximum adhesion.

So far, by applying also negative force triggers, we were able to interrupt the 'standard' adhesion process and could show that the snap-in process is a) a robust and characteristic feature of bacterial adhesion and is b) mediated by cell wall macromolecules. To corroborate the experimental results and the hypothesised model, we performed Monte Carlo (MC) simulations.

Monte Carlo Simulations

The model for the MC simulations bases on the key assumption that cell wall macromolecules can be described as elastic springs that attach to the substratum (for details of the model cf. supplementary material). An MC-simulated standard force/distance curve is shown in Fig. 5. Since the density and composition of cell wall macromolecules and their response to external forces is not known, there are many adjustable parameters in the model. However, considering the simplicity of our modeling approach, the agreement between experiment and MC simulation is remarkable: The snap-in event starts in the simulations (cf. Fig. 5b), as

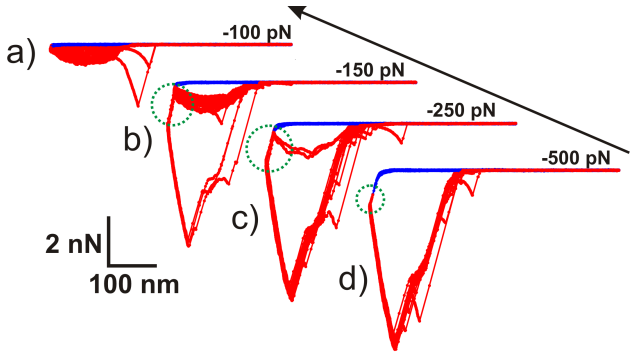

Fig. 4 'Partitioned' force/distance curves of a single *S. aureus* bacterial probe on a hydrophobised Si wafer for four different negative force triggers that allow for a stop of the approach at variable distances above the wafer surface. Each panel displays an overlay of 20 force/distance curves and were all taken with the exact same bacterium.

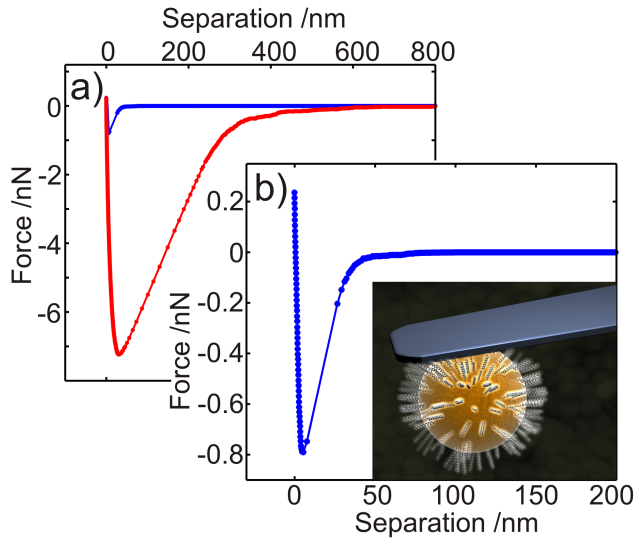

Fig. 5 Monte-Carlo-simulated standard force/distance curve, approach (retract) curve in blue (red). a) Entire curve, b) snap-in process of the simulated force/distance curve in more detail. The inset to b) schematically depicts the MC model where cell wall macromolecules are represented as elastic springs (objects are not to scale).

well as in the experiment (cf. Fig. 2b), with a small gradient which gets larger with decreasing distance until the snap-in force is reached.

Moreover, in the simulations as well, partitioned force/distance curves can be recorded using a negative force trigger (cf. Fig. 6). These curves also strikingly resemble the experimental curves, including the above described features, in particular features ii) and iii): The simulated curves exhibit a pulling regime, too, and partitioned force distance curves using a force trigger that is located in the low-gradient area only exhibit low adhesion forces like in the experiment (cf. experimental curves in Fig. 4a and simulated curves in Fig. 6a). As in the experiment, the number of simulated force/distance curves resembling the simulated standard force/distance curve increases with decreasing force trigger (cf. experimental curves in Figs. 4b-d and simulated curves in Figs. 6b-d). The simulated partitioned force/distance curves also show

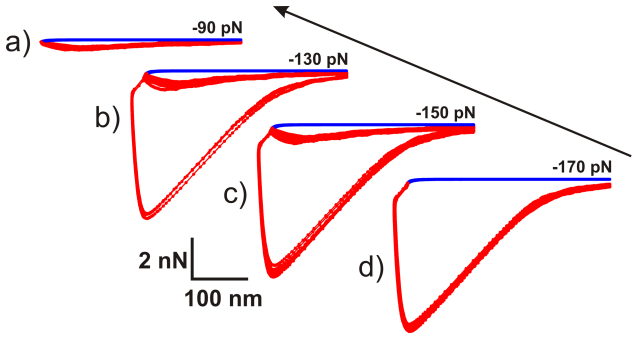

Fig. 6 Monte-Carlo-simulated partitioned force/distance curves for four different negative force triggers. Each panel displays an overlay of 20 simulated force/distance curves.

a sudden transition between low and high adhesion (pulling) regime. In experiments as well as in simulations, this transition occurs at force triggers located in the region where the gradient of the snap-in process in the standard force/distance curve features the strongest increase (cf. Fig. 2b and 5b). In other words, from the form of the snap-in event, one is able to predict the partitioned force/distance curves (within the inaccuracy due to the stochastic nature of the process).

Importantly, in the MC model, it is not sufficient to use just one sort of macromolecules (springs) with a given stiffness, rather, a spring constant distribution (cf. supplementary material) must be implemented for the macromolecules to reproduce the experimental features. The model now allows for a more detailed interpretation of the molecular processes during contact formation:

Due to thermal fluctuations and the structural heterogeneity of the cell wall proteins, a small number of proteins (the softer ones) initiate binding of the bacterium on approach, resulting in a small gradient of the force/distance curve. As the cantilever further reduces the distance to the substratum, more and also stiffer molecules can bind and the gradient of the force/distance curve becomes larger. These findings give rise to the assumption that different sorts of macromolecules with different properties are involved in the adhesion process.

All experimental force/distance curves shown in Figs. 1-3 were obtained with the identical bacterial probe. The described shape of the snap-in event, i.e. the increasing gradient for decreasing distances, is indeed characteristic of *S. aureus* single bacterial probes. The exact shape of the snap-in process, however, may vary for different *S. aureus* cells obtained from the same preparation. According to our results, we state that the actual appearance of the snap-in event of a single *S. aureus* bacterial probe is directly linked to the distribution and nature of the contact-forming cell wall macromolecules and that vice versa from the shape of the snap-in event it is possible to gather insight into the nature of the contact-forming macromolecules.

Protein-modifying treatment

To further evidence the macromolecular origin of the snap-in event and to explore the nature of cell wall macromolecules involved in the attachment process, we specifically modified prop-

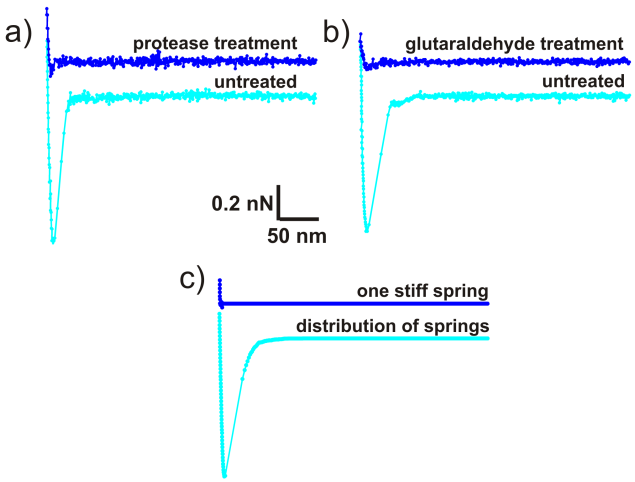

Fig. 7 Influence of enzymatic/chemical treatment on the bacterial snap-in process and its corresponding simulated force/distance curve. Snap-in event of a single *S. aureus* cell adhering to a hydrophobic Si wafer a) in its native state (cyan curve) and after treating the cell with protease, b) before (cyan curve) and after treating an *S. aureus* cell with glutaraldehyde. c) Simulated force/distance curves using a model bacterium covered with a large number of springs with stiffnesses distributed over a certain range (cyan curve) and with only one stiff spring (blue curve). The baselines of the blue curves have been shifted in y-direction by 0.2 nN.

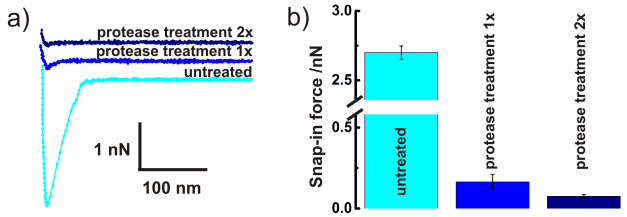

Fig. 8 Influence of two consecutive protease treatments on the bacterial snap-in process of an *S. aureus* cell, the baseline of the blue (dark blue) curve has been shifted in y-direction by 0.4 nN (0.8 nN) a). Recorded snap-in force for the untreated, one time and two times with protease treated *S. aureus*.

erties of cell wall proteins: We therefore treated the bacterial surface with two different protein-altering compounds, pronase E (Sigma-Aldrich) and glutaraldehyde (25% v/v, Sigma-Aldrich). Pronase E degrades proteins by cutting peptide bonds, whereas glutaraldehyde reacts with several functional groups of proteins and crosslinks them that way.[29,30] Thus, if driven by cell wall proteins, both treatments should significantly influence the snap-in process.

For these measurements, bacterial probes were prepared as described before, and prior to the enzymatic or chemical treatment, 20 force/distance curves were recorded on a hydrophobised Si wafer as a reference (Figs. 7a and b each show one reference approach curve for a force trigger of 300 pN). After that, the probe holder with the bacterial probe was removed from the AFM head leaving a droplet of buffer around the tip. With a pipette, 20 μl of 100 μg/ml solution of protease (or 12.5% glutaraldehyde solution, respectively) was added to the buffer droplet. After 10 min, the droplet around the tip was carefully removed and replaced by a fresh drop of buffer solution. This droplet of buffer was exchanged another three times to remove as much of the protein-modifying compound as possible. Then, new series of force/distance curves were taken (representative curves are given in Figs. 7a, b).

The protease as well as the glutaraldehyde treatment caused a substantial reduction of the snap-in process: the snap-in distance contracted from more than 30 nm to less than 10 nm and the snap-in force decreased to only a few pN as compared to 800 pN in the reference curves (Fig. 7). By cutting peptide bonds, the non-specific protease mixture should gradually reduce the length of the cell wall-attached proteins, thereby decreasing their hydrodynamic radii which impairs the bacterial snap-in process. To test this, we observed the snap-in event in between and after two consecutive protease treatments that were both applied as described above (cf. Fig. 8): Indeed, a second treatment with protease caused an additional reduction of the snap-in force (cf. Fig. 8b). A similar effect is expected for the protein crosslinker glutaraldehyde, which should affect both the mobility and the flexibility of proteins, thereby suppressing the stochastic process of tethering macromolecule by macromolecule to the surface. To capture the impact of a protein-modifying treatment, a rough model will give insight into the leading processes. As both treatments result in an increased stiffness of the macromolecules[31] and, at least, effectively in a decreased number of springs, we evaluated the force/distance curves of a model bacterium with only one single, stiff spring (spring constant of 1 N/m), in comparison to the model bacterium covered with a distribution of springs as described above, cf. Fig. 7c. The result is a simulated force/distance curve with only a tiny jump-to-contact (blue curve), instead of an extended snap-in process (cyan curve).

The retraction curves (see supplementary material) also featured a massive reduction in adhesion force and rupture length due to the enzymatic/chemical treatments respectively its model. However, for a detailed discussion of the detachment process, an in-depth knowledge of the molecular composition of the bacterial surface and the impact of the two protein modifying compounds would be needed, which is beyond the scope of this study.

Thus, by interfering with the length and the number or the mobility of the cell wall proteins, two important conclusions emerge: 1.) Cell wall proteins fulfill the major task in bacterial adhesion to hydrophobic surfaces and 2.) the consecutive tethering of cell wall proteins features major biological relevance as this mechanism strongly enhances the interaction range and strength between bacterium and surface. Simulated force distance curves support these findings.

3 Conclusions

The above results indicate why a general description of bacterial adhesion in the framework of the Derjaguin-Landau-Verwey-Overbeek (DLVO) theory or by the extended DLVO theory (including hydrophobic/hydrophilic interactions) fails if considered between the 'body' of the bacterium and the substratum. Actually,

the initiation of bacterial adhesion starts as far as 50 nm (sometimes even 100 nm) above the substratum, a distance, for which DLVO forces between the 'body' of the bacterium and the substratum are negligible.[3] Hence, the extended DLVO theory has to be applied to all cell wall macromolecules involved in the adhesion process. Our results indicate that on approach of a bacterium to a surface, a simple protein/surface potential allowing the proteins to bind is sufficient, while the number and the distribution of spring constants of the proteins are of importance. In other words, on contact formation, fluctuations in protein density and structure are much more relevant than the exact protein/surface binding potential.

To conclude, we studied and described the fundamental mechanisms of the initiation of contact during the adhesion of *S. aureus*. It has been demonstrated that the approach part of a force/distance curve can be reliably evaluated and characterises the initiation of adhesion comprehensively. MC simulations assuming bacterial cell wall macromolecules as elastic springs of different stiffness capture the observed experimental features of force/distance curves. An enzymatic/chemical treatment revealed that cell wall proteins dominate the attachment process and that disrupting the length of these molecules or their mobility causes severe changes in attachment. The proposed model and the resulting adhesion mechanism explain the observed force/distance curves of single cell bacterial probes as well as differences between varying bacterial species. Additional studies, e.g. using genetic tools to modify the bacterial cell wall composition, will allow to distinguish between the contributions of the different components/macromolecules. Applying a similar approach of single cell level experiments accompanied by molecular modeling onto entire force/distance curves, including both the approach and retraction parts, will pave the way to a global understanding of bacterial adhesion.

Acknowledgements

This work was supported by the Deutsche Forschungsgemeinschaft (DFG) within the collaborative research centre SFB 1027 and the research training group GRK 1276 (N.T.). M.B. was supported by grants of the German Ministry for Education and Research 01Kl1014B and 01Kl1301B.

References

1 A. E. Khoury, K. Lam, B. Ellis and J. W. Costerton, *ASAIO J.*, 1992, **38**, 174–178.

2 J. W. Costerton, P. S. Stewart and E. P. Greenberg, *Science*, 1999, **284**, 1318–1322.

3 K. Hori and S. Matsumoto, *Biochem. Eng. J.*, 2010, **48**, 424–434.

4 A. K. Epstein, T.-S. Wong, R. A. Belisle, E. M. Boggs and J. Aizenberg, *Proc. Natl. Acad. Sci. USA*, 2012, **109**, 13182–13187.

5 P. H. Tsang, G. Li, Y. V. Brun, L. B. Freund and J. X. Tang, *Proc. Natl. Acad. Sci. USA*, 2006, **103**, 5764–5768.

6 T. Das, B. P. Krom, H. C. van der Mei, H. J. Busscher and P. K. Sharma, *Soft Matter*, 2011, **7**, 2927–2935.

7 R. M. A. Sullan, A. Beaussart, P. Tripathi, S. Derclaye, S. El-Kirat-Chatel, J. K. Li, Y.-J. Schneider, J. Vanderleyden, S. Lebeer and Y. F. Dufrêne, *Nanoscale*, 2014, **6**, 1134–1143.

8 Y. Seo and W. Jhe, *Rep. Prog. Phys.*, 2008, **71**, 016101.

9 S. Kang and M. Elimelech, *Langmuir*, 2009, **25**, 9656–9659.

10 P. Loskill, H. Haehl, N. Thewes, C. T. Kreis, M. Bischoff, M. Herrmann and K. Jacobs, *Langmuir*, 2012, **28**, 7242–7248.

11 A. Beaussart, S. El-Kirat-Chatel, R. M. A. Sullan, D. Alsteens, P. Herman, S. Derclaye and Y. F. Dufrêne, *Nat. Protoc.*, 2014, **9**, 1049–1055.

12 *Handbook of Nanotechnology*, ed. Bhushan, Springer, 2004.

13 N. Thewes, P. Loskill, P. Jung, H. Peisker, M. Bischoff, M. Herrmann and K. Jacobs, *Beilstein J. Nanotechnol.*, 2014, **5**, 1501–1512.

14 S. Iordanescu and M. Surdeanu, *J. Gen. Microbiol.*, 1976, **96**, 277–281.

15 M. Lessel, O. Bäumchen, M. Klos, H. Hähl, R. Fetzer, M. Paulus, R. Seemann and K. Jacobs, *Surf. Interface Anal.*, 2015.

16 I. Maxe, C. Ryden, T. Wadström and K. Rubin, *Infect. Immun.*, 1986, **54**, 695–704.

17 A. Peschel, M. Otto, R. W. Jack, H. Kalbacher, G. Jung and F. Götz, *J. Biol. Chem.*, 1999, **274**, 8405–8410.

18 C. Weidenmaier, A. Peschel, Y.-Q. Xiong, S. A. Kristian, K. Dietz, M. R. Yeaman and A. S. Bayer, *J. Infect. Dis.*, 2005, **191**, 1771–1777.

19 S. Bur, K. T. Preissner, M. Herrmann and M. Bischoff, *J. Invest. Dermatol.*, 2013, **133**, 2004–2012.

20 J. L. Hutter and J. Bechhoefer, *Rev. Sci. Instrum.*, 1993, **64**, 1868–1873.

21 C. Heilmann, in *Bacterial adhesion*, ed. D. Linke and A. Goldman, Springer, 1st edn, 2011, ch. 7, pp. 105–123.

22 Z. Jaglic, M. Desvaux, A. Weiss, L. L. Nesse, R. L. Meyer, K. Demnerova, H. Schmidt, E. Giaouris, A. Sipailiene, P. Teixeira *et al.*, *Microbiology*, 2014, **160**, 2561–2582.

23 J. N. Israelachvili, *Intermolecular and Surface Forces*, Academic Press, 3rd edn, 2011.

24 C. A. Helm, J. N. Israelachvili and P. M. McGuiggan, *Biochemistry (Mosc.)*, 1992, **31**, 1794–1805.

25 E.-L. Florin, V. T. Moy and H. E. Gaub, *Science*, 1994, **264**, 415–417.

26 J. Y. Wong, T. L. Kuhl, J. N. Israelachvili, N. Mullah and S. Zalipsky, *Science*, 1997, **275**, 820–822.

27 D. Leckband and J. Israelachvili, *Q. Rev. Biophys.*, 2001, **34**, 105–267.

28 M. Rief, F. Oesterhelt, B. Heymann and H. E. Gaub, *Science*, 1997, **275**, 1295–1297.

29 I. Migneault, C. Dartiguenave, M. J. Bertrand and K. C. Waldron, *Biotechniques*, 2004, **37**, 790–806.

30 Y. Wine, N. Cohen-Hadar, A. Freeman and F. Frolow, *Biotechnology and bioengineering*, 2007, **98**, 711–718.

31 *Polymer Physics*, ed. M. Rubinstein and R. Colby, Oxford University Press, 1st edn, 2003, ch. 2, pp. 49–78.